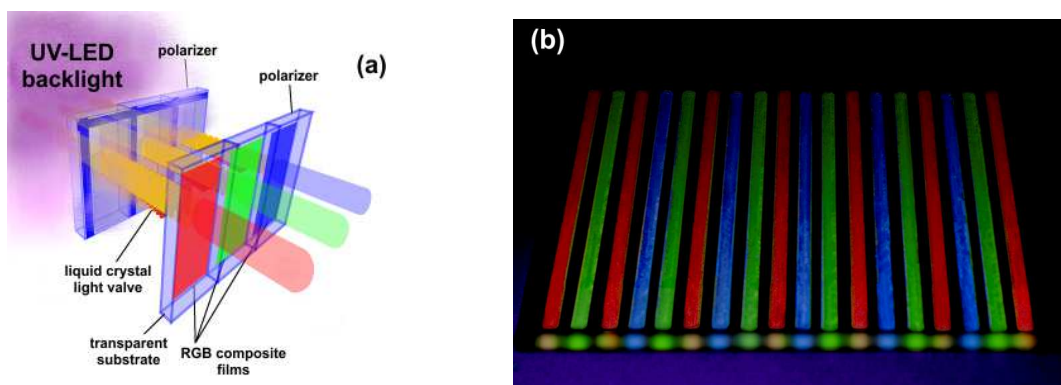


**Innovative electroluminescent nanocomposites for a new  
approach in polymer based light emitting devices**

project: 335/5.10.2011 **Stage IV** (2015)

**Scientific report**

In this research stage, activities were directed to obtaining thin composite films with emission in the three fundamental colors (R,G,B). the RGB intense emission of the prepared composites and their ability to be processed in thin or thicker films according with the application requirements may be usable in AMLCD displays. The composites could replace the usual RGB filters in a configuration which uses UV-LED's instead of white LED's for backlighting. A possible approach is presented in **Figure 1.a.** while in **Figure 1.b.** is presented an experimental study of alternating in line, spray coated RGB composites deposited on a transparent PMMA substrate.



**Figure 1.** (a) A possible approach for implementation in AMLCD; (b) Experimental study of spray coated RGB composites under UV-A excitation

The emissive properties of the prepared composites are relying essentially on the photoluminescence of the embedded complexes. The characteristic narrow band emission of the  $[\text{Eu}(\text{L})_3(\text{H}_2\text{O})_3]$  and  $[\text{Tb}(\text{L})_3(\text{H}_2\text{O})_3]$  complexes is based on a classic metal centered photoluminescence mechanism where the efficient sensitization provided by the surrounding ligands triggers radiative transitions within  $4f$  orbitals of the central cation. In case of the  $[\text{Y}(\text{L})_3(\text{H}_2\text{O})_3]$  complex the intense, wider band blue emission is governed by a different mechanism which involves the influence of the heavy atom vicinity over the excited states of the ligands. Through embedding in the PVA and PVP matrices, the luminescent properties of the complexes are favorable affected in terms of emission efficiency and spectral purity. As mentioned above, the new environment provided by the polymer matrices and the interactions occurrence between functional

groups, could play the main roles in the observed enhancements of the photoluminescent properties. In **Figure 2.a** are presented the excitation/emission spectra of the prepared PVA-[Eu(L)<sub>3</sub>(H<sub>2</sub>O)<sub>3</sub>] and PVP-[Eu(L)<sub>3</sub>(H<sub>2</sub>O)<sub>3</sub>] composites while for comparison, the excitation/emission spectra of the free complex, is also included. In all cases, the transitions responsible for the recorded emission peaks are as follows: the <sup>5</sup>D<sub>0</sub>→<sup>7</sup>F<sub>1</sub> for the 589-591 nm peaks; <sup>5</sup>D<sub>0</sub>→<sup>7</sup>F<sub>2</sub> for the 613-616 nm peaks; the low intensity peaks located at 640 and 650 visible only in the PVA composite and free complex spectra are due to the <sup>5</sup>D<sub>0</sub>→<sup>7</sup>F<sub>3</sub> transition; <sup>5</sup>D<sub>0</sub>→<sup>7</sup>F<sub>0</sub> transition is responsible for the barely observable 576-578 nm peaks. The <sup>5</sup>D<sub>0</sub>→<sup>7</sup>F<sub>1</sub> parity-allowed magnetic dipole transition responsible for the peak centered around 590 nm is practically unaffected by the surroundings symmetry while the most intense 615 nm centered peaks due to the <sup>5</sup>D<sub>0</sub>→<sup>7</sup>F<sub>2</sub> electrical-dipole allowed hypersensitive transition is known to be highly affected by surrounding symmetry degree. The ratio between the emission intensities of these two peaks is an asymmetry parameter for the Eu<sup>3+</sup> surroundings, higher values indicating lower symmetry configurations. As could be noted, through embedding in the PVA matrix the intensity ratio between the 615 and 591 nm peaks is almost 2 while for the case of the free complex the intensities of these two peaks being practically equal. In case of the PVP composite the ratio between the 613 and 590 nm peaks is ~ 3.2 indicating an even more disordered configuration of the Eu<sup>3+</sup> surroundings. From the practical perspective, the most favorable situation is achieved in case of the PVP-[Eu(L)<sub>3</sub>(H<sub>2</sub>O)<sub>3</sub>] composite where the dominant 613 nm peak provide a photoluminescent emission with higher level of chromatic purity, thus allowing a “deeper” red (Figure 3.b) in the targeted applications.

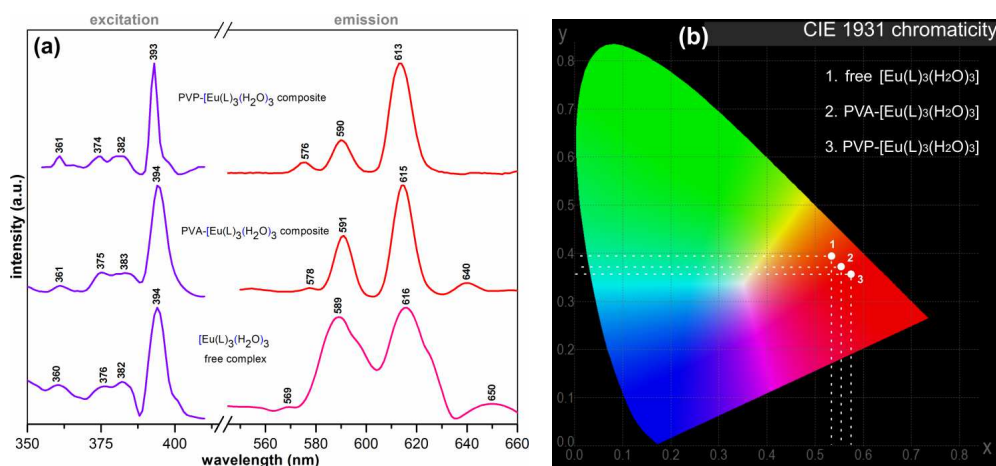


**Figure 2. a.** Excitation/emission spectra recorded for the [Eu(L)<sub>3</sub>(H<sub>2</sub>O)<sub>3</sub>], PVA-[Eu(L)<sub>3</sub>(H<sub>2</sub>O)<sub>3</sub>] PVP-[Eu(L)<sub>3</sub>(H<sub>2</sub>O)<sub>3</sub>], **b.** CIE 1931 chromaticity parameters

**Figure 3.a** presents the excitation/emission spectra of the prepared PVA-[Tb(L)<sub>3</sub>(H<sub>2</sub>O)<sub>3</sub>] and PVP-[Tb(L)<sub>3</sub>(H<sub>2</sub>O)<sub>3</sub>] composites and also for the free complex. As could be noted, in their case the emission spectra are similar in all cases, the recorded peaks being the result of the following radiative transitions: <sup>5</sup>D<sub>4</sub>→<sup>7</sup>F<sub>5</sub> is responsible for the most intense peak located at 542-544 nm,

$^5D_4 \rightarrow ^7F_6$  for the medium intensity peak located at 487-488 nm while the  $^5D_4 \rightarrow ^7F_4$  and  $^5D_4 \rightarrow ^7F_3$  transitions are responsible for the 582-583 nm and 619-620 nm lower intensity peaks.

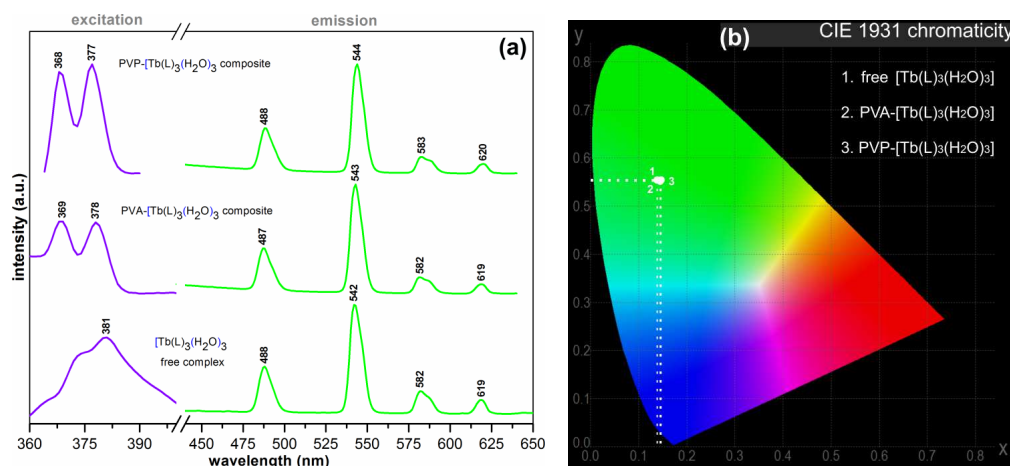


**Figure 4.a.** Excitation/emission spectra recorded for the [Tb(L)<sub>3</sub>(H<sub>2</sub>O)<sub>3</sub>], PVA-[Tb(L)<sub>3</sub>(H<sub>2</sub>O)<sub>3</sub>], PVP-[Tb(L)<sub>3</sub>(H<sub>2</sub>O)<sub>3</sub>], **b.** CIE 1931 chromaticity parameters

In case of the PVA-[Y(L)<sub>3</sub>(H<sub>2</sub>O)<sub>3</sub>] and PVP-[Y(L)<sub>3</sub>(H<sub>2</sub>O)<sub>3</sub>] composites (**Figure 5**) several interesting modifications were observed in their recorded spectra (Figure 4.a) when compared with the free complex. The intense, wider band emission peaks arising from the intraligand radiative transitions are displaced to lower wavelengths (from 482 to 472-474 nm) allowing a “deeper” blue emission (**Figure 5.b**) which is also favorable for the targeted applications. The most important modification appears in the excitation spectra where an important shift of the excitation peak was recorded. This is very important from the applications perspective since the excitation peaks of the RGB emissive composites are situated in a narrow 375-390 nm range, therefore being possible to be efficiently excited by just one type of source, for ex. 375, 380 nm UV-LED’s. The situation is especially available in case of the prepared PVP composites where the additional advantages of higher absolute PLQY and spectral purity making them better suited for the targeted applications.

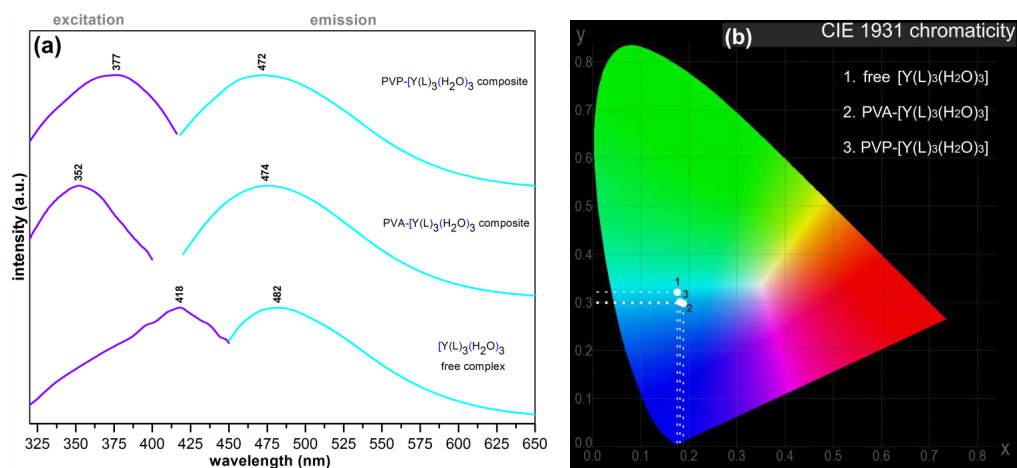


**Figure 5. a.** Excitation/emission spectra recorded for the [Y(L)<sub>3</sub>(H<sub>2</sub>O)<sub>3</sub>], PVA-[Y(L)<sub>3</sub>(H<sub>2</sub>O)<sub>3</sub>], PVP-[Y(L)<sub>3</sub>(H<sub>2</sub>O)<sub>3</sub>], **b.** CIE 1931 chromaticity parameters

The absolute PLQY values recorded at several excitation wavelengths are presented in Table 1. The highest values are achieved by the PVA –[Tb(L)<sub>3</sub>(H<sub>2</sub>O)<sub>3</sub>] and PVP –[Tb(L)<sub>3</sub>(H<sub>2</sub>O)<sub>3</sub>] and the overall results are better in case of all PVP composites.

**Table 1.** recorded absolute PLQY values for the prepared composites

$\lambda$ excitation (nm)	Absolute PLQY (%)					
	PVA – [Tb(L) <sub>3</sub> (H <sub>2</sub> O) <sub>3</sub> ]	PVA - [Eu(L) <sub>3</sub> (H <sub>2</sub> O) <sub>3</sub> ]	PVA - [Y(L) <sub>3</sub> (H <sub>2</sub> O) <sub>3</sub> ]	PVP - [Tb(L) <sub>3</sub> (H <sub>2</sub> O) <sub>3</sub> ]	PVP - [Eu(L) <sub>3</sub> (H <sub>2</sub> O) <sub>3</sub> ]	PVP - [Y(L) <sub>3</sub> (H <sub>2</sub> O) <sub>3</sub> ]
350	54,81	36,90	<b>47.16</b>	-	-	-
360	61,96	41,04	43.50	53.55	44.61	38.79
370	<b>67.54</b>	51,22	38.53	61.11	49.10	47.03
380	-	53.17	33.28	<b>69.21</b>	53,81	<b>52.41</b>
390	-	<b>58.49</b>	-	-	<b>59,09</b>	-

The recorded AFM images highlighted the presence of submicronic structures relatively uniform dispersed in the polymer matrices suggesting the presence of the clustered complexes. In Figure 7 are presented the AFM images recorded for the prepared PVA-[Eu(L)<sub>3</sub>(H<sub>2</sub>O)<sub>3</sub>] composite and PVP-[Tb(L)<sub>3</sub>(H<sub>2</sub>O)<sub>3</sub>] respectively. These AFM images are also typical for the rest of the prepared composites, no notable differences being visible in their cases.

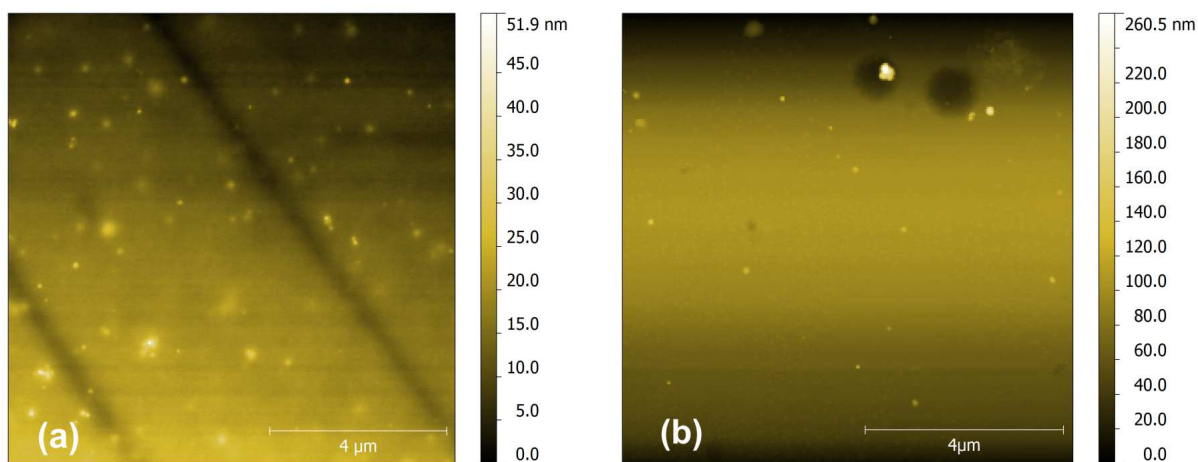


**Figure 7.** AFM images recorded for the (a) PVA –[Eu(L)<sub>3</sub>(H<sub>2</sub>O)<sub>3</sub>],  
(b) PVP –[Tb(L)<sub>3</sub>(H<sub>2</sub>O)<sub>3</sub>] composites

In case of the PVP composites the dimensions of the clustered complexes are slightly lower with an average diameter in 100-200 nm range while in case of the PVA composites the average diameter being in 300-500 nm range. These particularities are also visually detected by a more homogenous, transparent and glossier aspect of the PVP composites.